Positronium desorption of positrons bound to alkali-metal-covered Ni surfaces

D. W. Gidley and A. R. Köymen*
Department of Physics, University of Michigan, Ann Arbor, Michigan 48109-1120

T. W. Capehart
Physics Department, General Motors Research Laboratories, Warren, Michigan 48090-9055
(Received 22 June 1987)

Both positrons and electrons can be bound to metal surfaces by image-correlation interactions. For electrons, the image potential dominates, preventing the electron from escaping into vacuum. For positrons, a consistent picture of the trapping process has not been developed. We investigate the effect of alkali-metal-atom adsorption on the binding of positrons to Ni surfaces. Thermal desorption of positronium is observed for temperatures down to 325 K and cryogenic desorption is predicted. The slow variation of the activation energy for positronium desorption with alkali-metal-atom coverage indicates that correlation effects dominate the positron surface state. The physical picture considered is that of a composite particle trapped in a correlation well of the screened positron with the well eventually joined to the 1*s* positronium bound state.

I. INTRODUCTION

Thermal positrons diffusing back to the surface are trapped in surface states on a number of metals. This surface trapping was first deduced from the observation that the positron could be thermally desorbed from the surface at elevated temperatures as a bound electron-positron pair, positronium.[1-4] Such desorption as positronium (Ps) is energetically favored over bare positron desorption because the Ps binding energy gained in capturing an electron (6.8 eV) is larger than the electron work function, ϕ_-, in metals. Experimentally it is found that as the sample temperature increases the temperature activated Ps component becomes comparable to the temperature independent "direct" channel. This doubling of the Ps formation fraction results in 60–100 % of the positrons diffusing back to the surface being emitted as Ps. Analysis of the temperature-dependent component permits an accurate determination of the activation energy, E_a, for the Ps desorption process. Utilizing the Born-Haber cycle,

$$E_a=\phi_-+E_b-6.8\ \text{eV}\ , \tag{1}$$

the binding energy, E_b, of a *bare positron* bound to a surface has been deduced for a number of metal surfaces.[2-5] Typical values of E_b are 2–3 eV.

These deduced binding energies are certainly too large to be understood as a bare positron trapped on the vacuum side by an image potential and on the crystal side by a hard wall. The expected binding energies in such an image well form a Rydberg-like series,[6]

$$E_n=(0.85\ \text{eV})/(n+a)^2,\quad n=1,2\ldots\ , \tag{2}$$

with $a=0$. Indeed, the extrinsic electron surface states binding energies are measured[7] to be $\lesssim 0.85$ eV, in quantitative agreement with this image potential model.

The lack of correspondence between the positron and electron surface states indicates a more subtle origin for the positron states than the image potential which produces the relatively simple Rydberg-like spectrum of extrinsic electron surface states. This fact was recognized[8,9] even before the surface bound positrons were observed in desorption experiments. The effect of electron-positron correlation close to the metal surface was incorporated in the theory to provide a broader "image-correlation" well with higher binding energies, E_b. The measured values of E_b are in quite reasonable agreement with the calculated results.[10-12] Recent experiments have investigated the positron lifetime in surface states,[13] and the angular correlation of the γ rays produced by the positron-electron annihilation at the surface.[14] These results are not consistent with predictions[9,12] based on the image-correlation well models.

Recently, Platzman and Tzoar have proposed an alternative model of these states viewing them as Ps, a highly correlated positron and electron, physisorbed to a metal surface by the van der Waals interaction.[15] The width of the truncated van der Waals well is empirically selected to produce a Ps binding energy in the well [E_a in Eq. (1)] that is consistent with the measurements. The positron lifetime predicted by this work is in good agreement with the measured values,[13] and results reported in the present paper (preliminary results were reported in brief form in a conference proceeding[16]) were noted to be in qualitative agreement. This model was not, however, able to reproduce the observed angular correlation.[15] And, while it is a valuable model, the ability to extend the van der Waals model to quantitatively treat the positron-surface interaction within several Å of the surface is questionable. A central element to such a treatment is a constant promotion energy (the energy difference between the 1*s* and 2*p* binding energies of Ps). Lowy and Jackson have shown[17] however that the 1*s* state merges with the continuum (and hence the promotion energy vanishes) at electron densities found as far as several Å outside a metal surface. Other theoreti-

 ©1988 The American Physical Society

cal treatments have been developed[18–20] but they are sufficiently complex to prevent ready comparison with the present experiments. In short, there is no clear consensus as to the nature of these positron/Ps surface states.

In order to clarify the character of the positron surface states we have systematically investigated the dependence of E_a [and hence E_b in Eq. (1)] on a wide range of electron work function values, ϕ_-, by depositing submonolayer amounts of an alkali metal on Ni single crystals. Specifically, we have investigated the formation of Ps for deposits of Li, Na, K, or Cs on Ni(100), and Cs on Ni(110) for a range of substrate temperatures using a low-energy spin-polarized beam of positrons.

Two reasons motivated the selection of simple metal adsorbates: First, if we naively assume E_b is universally 2–3 eV, then inspection of the Born-Haber cycle suggests that E_a should depend sensitively on ϕ_-. Reduction of ϕ_- by several eV occurs on Ni at coverages of a fraction of a monolayer of the alkali metals. The attendant reduction in E_a from typically 0.5 eV to nearly zero should require no more than 0.1 monolayer coverage and would provide the first cryogenic source of Ps with kinetic energies corresponding to room temperature or below.[21] (Such a source would be useful in a number of Ps lifetime and spectroscopy experiments.) Second, there has been no systematic investigation of positron trapping and Ps formation on the simple metals. The alkalis are unique because of their low ϕ_- and high predicted[22] positron work function ($\phi_+ \simeq 5$ eV). As a result it is expected that no positron surface state exists on the alkali metals.[22] However, in this work we demonstrate that Ps desorbs from the alkali covered Ni surface, measure its activation energy, E_a, and Ps desorption kinetic energy. And while E_a can be lowered by the requisite 0.5 eV to nearly zero, it is surprising that a half-monolayer alkali coverage with an attendant decrease of 3–3.5 eV in ϕ_- is required. We deduce from Eq. (1) that $E_b \cong 5$ eV for this surface, nearly twice as large as any previously reported value of E_b. This result is difficult to reconcile with the image-correlation well model.

The unexpectedly large binding energy E_b for the positron surface states and the insensitivity of E_a to changes in the electron work function are intertwined. Together they suggest a needed reevaluation[15,19] of the physical picture of the positron/Ps surface state. In order to provide a simple framework for interpreting our experimental results we adapt the effective medium theory of Nørskov and Lang[23] applied to the positron (i.e., the Ps^+ ion) in lowest order. Although calculated only to lowest order, our development is virtually free of empirically chosen parameters. The central ideas of our treatment are (1) Ps desorbs as a neutral—this is the physical channel, the image potential at long range is irrelevant to the trapping potential, (2) the stabilization energy of Ps^+ is given by the positron-electron correlation energy as calculated by Bhattacharyya and Singwi.[24]

The above assumptions lead to a model that can be physically pictured as intermediate between the limiting cases of the single channel models (positron trapping versus Ps trapping). We model the trapped particle as a highly correlated positron and electron. Near the surface the positron has a screening cloud composed of electron states from the metal. As the positron moves away from the surface this screening cloud is slowly replaced by the Ps 1s state. Solutions of the Schrödinger equation for the composite model potential provide the binding energy of the particle. Finally, the polarization of the correlated positron and electron produced by the dipole field in the surface region is considered.

Though this development is different, the character of the surface state—a screened, polarized composite particle—is similar to the result obtained by Cuthbert[20] using a hydrodynamic model in which short-range correlation is included by the introduction of a single distinguishable electron. The advantage of the present approach for us is its physical simplicity which permits ready comparison to the experimental results. As will be seen in the final section, the relatively good agreement found in this lowest-order approach warrants a more serious treatment with the inclusion of higher-order terms.

In the next section experimental techniques will be discussed. Subsequent sections will present the following results: Ps thermal desorption curves, measurements of the kinetic energy of the desorbed Ps, and isotherms of Ps formation versus alkali coverage. In the concluding section the results are analyzed and a model of the positron surface state is developed. An Appendix discusses the effect of alkali-metal-atom adsorption on the spin polarization of the Ni surface.

II. EXPERIMENTAL APPARATUS

The low-energy (and spin-polarized) positron beam has been previously described.[25,26] The positrons with energy fixed at 900 eV are electrostatically focused onto the Ni sample (see Fig. 1). The sample is held in a C-shaped electromagnet that is used to magnetically saturate the Ni in the spin polarized experiments (see Appendix).

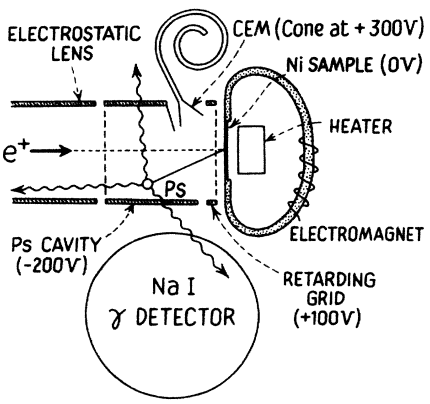

FIG. 1. Schematic diagram of the experimental arrangement showing the electrostatic lenses, Ps cavity, sample holder, γ detector, and channel electron multiplier (CEM).

The rate of electron capture to form triplet (long-lived) Ps is measured using either lifetime or γ-ray pulse-height techniques. Lifetime spectra are acquired using a conventional time-to-amplitude converter/multichannel analyzer system. Start and stop signals are derived from the detection of secondary electrons in a channeltron (CEM) ejected by the incident 900 eV positron and the subsequent detection of an annihilation γ ray in the NaI scintillator, respectively. The Ps formation fraction, f, is determined from the ratio of the long-lived events (between 30 and 405 ns) and the total number of events in the background-corrected lifetime spectrum.[25] In a 5 min run f can be measured to a statistical accuracy of about 0.5%. There is an overall systematic error of 5% in determining f from the ratio of counts in the lifetime spectrum. As an alternative to the lifetime technique, f could be measured by analyzing the pulse-height spectrum from the NaI γ-ray detector. Decay of triplet Ps into 3 γ rays can be observed as a sizable increase in the 511 keV Compton valley-to-511 keV peak counting rate ratio (see Refs. 25 and 26 for further details). This pulse-height technique was used for several runs at high sample temperature (>300 °C) at which thermally generated noise rates in the CEM were too high for the timing system.

The uhv target chamber is equipped with a double-pass cylindrical mirror analyzer for Auger electron spectroscopy and four-grid LEED optics for low-energy electron diffraction. The Ni(110) and Ni(100) samples were cleaned by repeated cycles of 2-keV Ar ion bombardment, annealing to 900 °C, and flash desorption of oxygen at 600 °C. On the Ni(100) surface we exposed the heated sample to just enough oxygen to remove the carbon Auger peak by monitoring both peaks during oxygen dosing. No appreciable contaminants were then observed in the Auger spectra acquired at room temperature.

An externally heated Knudsen cell was used for high-purity Cs evaporation while resistively heated alkali getters were used to evaporate K, Na, and Li. Coverage is determined by measuring the Cs (563 eV), K(250 eV), or Na (990 eV) Auger peak-to-Ni (848 eV) peak ratio. An estimate of the Auger ratio corresponding to one physical monolayer is determined using electron mean free paths calculated by Penn.[27] To determine the Li coverage we monitored the attenuation of the Ni (102 eV) Auger peak during Li depositions. As a result the Li coverage is much more susceptible to systematic error than the other coverage determinations. Additional evidence helped to corroborate our coverage calibration for some of the alkalis. The Cs and K surfaces at 50 °C appear to form only one monolayer[28] (the second layer being inhibited by the high vapor pressure of Cs and K) and thus a consistent upper limit in the Cs and K Auger peaks is observed. Na on Ni(100) forms a $c(2\times2)$ structure at one physical monolayer[28,29] and this LEED pattern was clearly evident. In addition, slight heating (to 90 °C) of high Na coverage surfaces always produced an Auger ratio near 0.042 along with the $c(2\times2)$ structure, indicating desorption of all but the first monolayer. Finally, for all four alkalis on Ni(100) the change in the electron work function, $\Delta\phi_-$, is measured at the same coverage at which Ps formation is measured. The LEED electron gun is used to measure $\Delta\phi_-$ and in each case the $\Delta\phi_-$ versus coverage curves are in excellent agreement with previous determinations.[29-31]

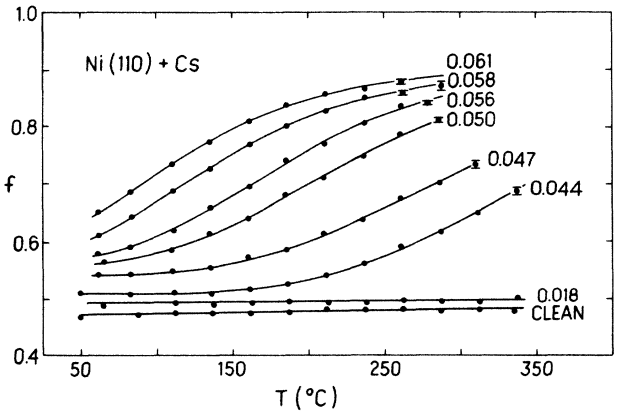

FIG. 2. Temperature dependence of the Ps fraction, f, at several Cs coverages indicated by the measured ratios of the Cs 563 eV Auger peak to the Ni 848 eV peak ($\Theta=1$ corresponds to 0.15). The solid line is a fit to the thermal desorption theory [see text, Eq. (3)].

III. THERMAL DESORPTION OF POSITRONIUM

To determine the kinetic parameters of the positron surface states we measured the Ps formation fraction f as a function of substrate temperatures for various Cs coverages on Ni(110) and Na coverages on Ni(100). These data, shown in Figs. 2 and 3, clearly indicate that a thermally activated, coverage dependent process is responsible for the increase in f. A single desorption curve (not shown) was also acquired for Cs on Ni(100) and K on Ni(100) as a check for consistency. These data, acquired using the lifetime technique, are limited

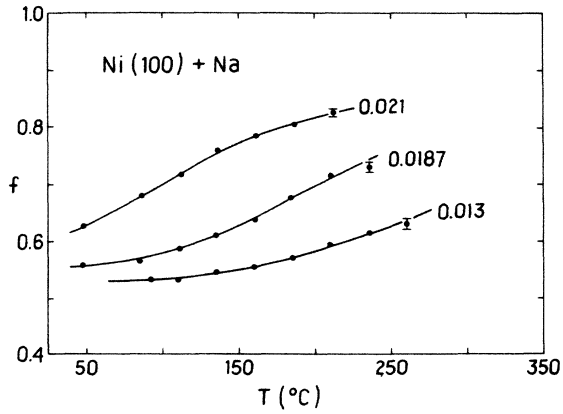

FIG. 3. Temperature dependence of the Ps fraction, f, at several Na coverages indicated by the measured ratios of the Na 990 eV Auger peak to the Ni 848 eV peak, as in Fig. 2 ($\Theta=1$ corresponds to 0.042). The solid lines are fits to Eq. (3).

to a maximum substrate temperature of about 300 °C by noise in the CEM start signal. To clearly demonstrate the desorption processes involved we acquired data over an extended temperature range using the pulse-height technique. As shown in Fig. 4, it can be seen that roughly 0.3 monolayers of Cs on Ni(110) reduces the temperature (presumably by reduction of E_a) at which Ps thermal desorption occurs by about 500 °C. As the Cs desorbs from the surface between 400 °C and 600 °C, f drops as E_a increases back to the clean surface value. The Ps fraction then begins to rise again as thermal desorption from the clean surface is activated. Ps desorption from clean Ni(100) has previously been observed[4] to occur at about 900 °C, in reasonable agreement with our observations on the Ni(110) surface.

We now turn to a more quantitative treatment of the thermal desorption data presented in Figs. 2 and 3. It is assumed that the Ps desorption rate is $\nu e^{-E_a/kT}$ and thus the temperature-dependent Ps formation fraction is expected to be[1-5]

$$f(T)=f(0)+[f(\infty)-f(0)][1+(\lambda/\nu)e^{E_a/kT}]^{-1}, \quad (3)$$

where λ is the decay rate of the positron in the surface state and $f(0)$ and $f(\infty)$ are the low- and high-temperature limits of $f(T)$. The desorption spectra were fitted to Eq. (3) and the resulting curve is shown as the solid line in these figures. The χ^2 of the fits ranged uniformly from 2–14 for seven or eight degrees of freedom. We have taken the exponential prefactor to be a temperature-independent constant. It is actually expected that ν should follow a power-law dependence on T with the exponent determined by the dimensionality of the surface well.[5] However, refitting the data with T and $T^{3/2}$ functions for ν failed to distinguish a preferred exponent.

The fitted values of E_a, $f(0)$, and $f(\infty)$ for Cs on Ni(110) are shown in Fig. 5 along with the corresponding values for Na on Ni(100). We note that $f(\infty)$ is nearly constant with coverage indicating a complete conversion of positrons to Ps. Consistent with a slight increase in direct (temperature independent) Ps formation with increasing coverage, $f(0)$ increases as will also be shown in Sec. V. The fitted values of λ/ν varied randomly from 5×10^{-5} to 5×10^{-4} and thus, with no apparent trend evident in this parameter, we refit the data with average values of $(\lambda/\nu)=2\times10^{-4}$ and 4×10^{-4} for the Na and Cs data, respectively. This tends to smooth the E_a results somewhat, which are seen in the figure to uniformly decrease with coverage. Linearly extrapolating E_a to zero coverage yields 0.84±0.1 eV for Ni(110) and 0.64±0.1 eV for Ni(100). The agreement of the Ni(100) intercept with a previous measurement[4] of E_a for clean Ni(100) tends to support a roughly linear dependence on E_a with alkali coverage. At higher coverages our inability to cool the sample prevented us from measuring E_a directly for $\Theta>0.5$. However, assuming the linear extrapolation of E_a shown in the figure we estimate that spontaneous Ps desorption ($E_a=0$) would occur at $\Theta=0.7$ for Cs on Ni(110) and $\Theta=0.9$ for Na on Ni(100). Thus on a cooled cesiated surface, the range $0.5<\Theta<0.7$ should be suitable for producing "cryogenic" Ps, i.e., Ps with an average kinetic energy corresponding to room temperature or below. The implications of these results will be considered in greater detail in Sec. V.

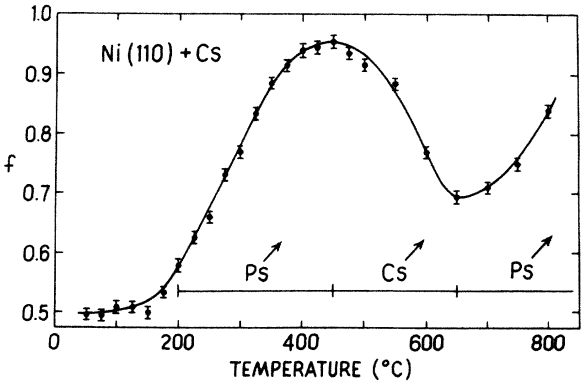

FIG. 4. Temperature dependence of the Ps fraction, f, over an extended temperature range using the pulse-height technique. The Cs-to-Ni Auger ratio at the beginning of the temperature ramp corresponds to about one-third of a monolayer. In sequence the data show the room-temperature desorption of Ps from the cesiated surface, the desorption of Cs which increases E_a, and finally desorption of Ps from the clean Ni surface above 650 °C.

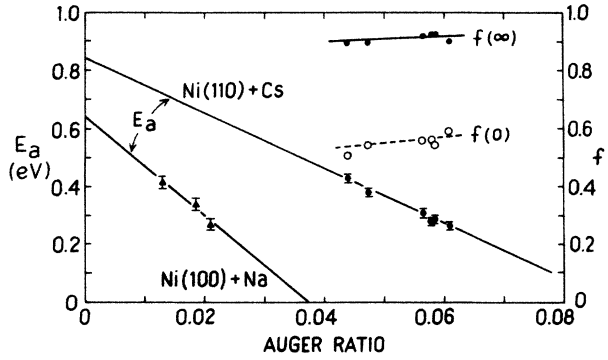

FIG. 5. Fitted parameters from the desorption equation [Eq. (3)] for Cs on Ni(110) and Na on Ni(100) for different alkali-metal–Ni Auger ratios. Note the nearly linear dependence of E_a with the Auger ratio.

IV. KINETIC ENERGY OF DESORPTION

As a check that cesiated Ni is a source of low energy Ps, we have indirectly measured the average kinetic energy of the desorbed Ps. We anticipate[21] the thermally desorbed component of the triplet Ps fraction to have a thermal energy distribution characteristic of the desorption temperature (e.g., about 0.06 eV at 200 °C). The average Ps emission energy can be deduced from the increase in the measured decay rate in the annihilation lifetime spectrum, λ_0, by noting that the value of λ_0 is expected to be

$$\lambda_0=\lambda+\gamma v \ , \tag{4}$$

where λ is the vacuum decay rate (7.05 μsec^{-1}) of triplet Ps and v is the average Ps velocity. The parameter γ is a geometry-dependent constant that accounts for the collisional quenching of Ps at the surface of the stainless-steel lenses (see Fig. 1) as well as the disappearance of Ps from the viewing region of the γ-ray detector.[32] We assume that the characteristic energy of Ps directly emitted from a clean Ni(110) surface is roughly equal to $-\phi_{Ps}$ (about 3 eV) (Ref. 33) and that this produces the observed increase in the measured decay rate from the vacuum value to approximately 10.2 μsec^{-1}. The annihilation decay rate of thermally desorbed Ps may be obtained by subtracting suitably normalized high- and low-temperature spectra acquired at the same Cs coverage. With the 1-in.-long and 1-in.-diameter stainless-steel confinement cavity used, we measured $\lambda_0=10.2$ μsec^{-1} when the sample is below the desorption temperature T_D. Heating the target above T_D and subtracting spectra produced a difference spectrum in which the existence of a single exponential with $\lambda_0=7.2\pm0.2$ μsec^{-1} (i.e., almost no collisional quenching or disappearance) is taken as evidence of thermal energy Ps being emitted from the surface. Using the above data for Cs on Ni(110) and Eq. (4) we deduce a Ps kinetic energy of $0.01+0.4$ or -0.01 eV, in reasonable agreement with a strictly thermal energy distribution.

V. ISOTHERMAL DESORPTION

In Fig. 6 the measured values of f as a function of Cs coverage on Ni(110) are shown. In this curve ϕ_- was not measured. Similar curves for all four alkali metals on Ni(100) are shown in Figs. 7–10 along with the concomitantly measured values of $\Delta\phi_-$. In all figures a sharp rise in the Ps formation fraction occurs near $\Theta=0.5$ where ϕ_- reaches a broad minimum. Consistent with the thermal desorption spectra in Sec. III we interpret this increase in f to the onset of rapid thermal desorption (at 50 °C) of Ps from a surface bound state.

There is significant scatter in the Ps fraction data which we attribute largely to the sensitivity of the data to surface contamination.[29] The getters tended to produce CO and the amount of contamination depended on how new or well outgassed the getters were. The contamination problem seemed to be most acute when dos-

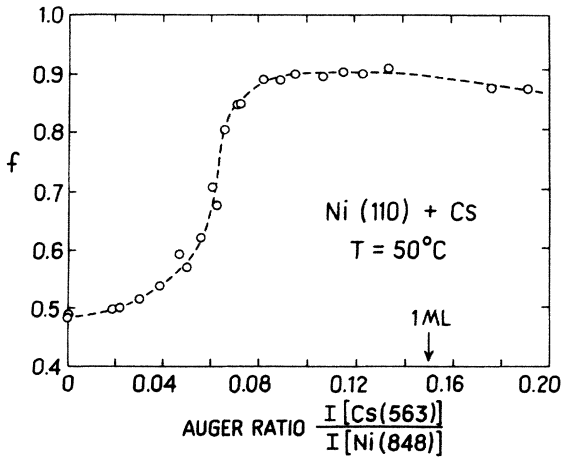

FIG. 6. Isothermal desorption of Ps at $T=50$ °C as the Cs coverage is varied from 0 to 1.25 monolayers (ML) on Ni(110). The dashed line is included to guide the eye.

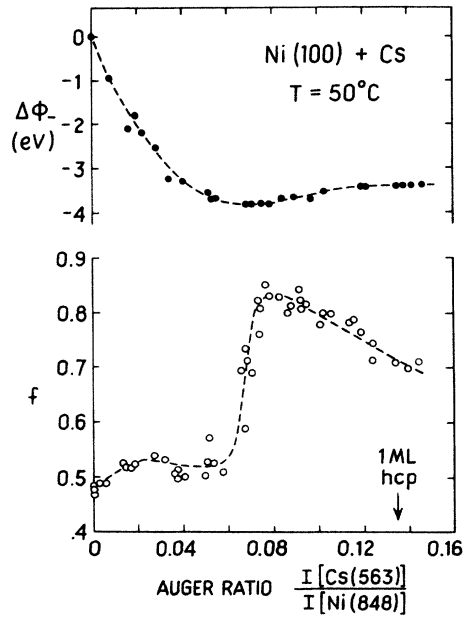

FIG. 7. Isothermal desorption of Ps and the change in the electron work functions, $\Delta\phi_-$, at $T=50$ °C as the Cs coverage is varied from 0 to 1.0 monolayer on Ni(100).

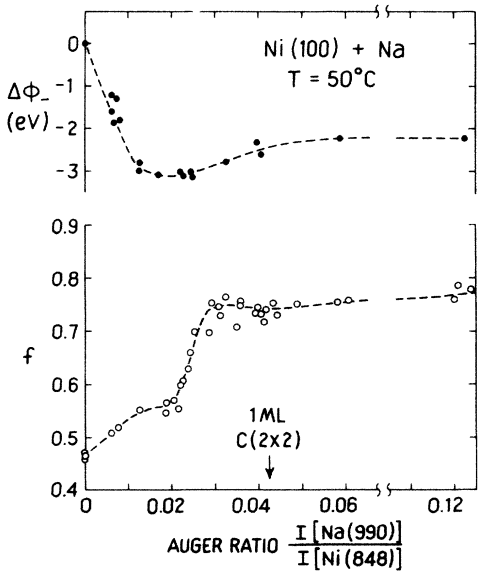

FIG. 8. Isothermal desorption of Ps and the change in electron work function, $\Delta\phi_-$, at $T=50$ °C as the Na coverage is varied from 0 to 3.0 monolayers on Ni(100).

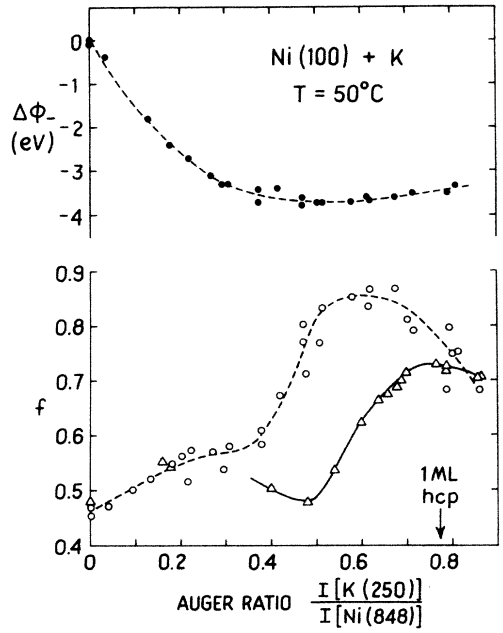

FIG. 9. Isothermal desorption of Ps and the change in electron work function, $\Delta\phi_-$, at $T=50$°C as the K coverage is varied from 0 to 1.0 monolayer on Ni(100). Open circles: some O_2 contamination observed. Triangles: negligible contamination (see discussion in Sec. V).

ing K. In Fig. 9 two curves of f have been plotted: the upper curve (open circles) which was taken concomitantly with the $\Delta\phi_-$ curve showed some oxygen contamination (presumably from CO), and the lower curve was acquired using a rebuilt evaporator that produced K with negligible contamination. Although the clean K surface has roughly the same jump in f, the curve is skewed downward to the right. The Li data show even greater fluctuations due to the uncertainty in calculating coverage from the Ni(102 eV) Auger line. The $\Delta\phi_-$ data for Li have been plotted versus coverage, where Θ has been determined from the Auger data. This technique is least sensitive at low Θ, as seen in the large scatter in the data for $\Delta\phi_-$. We have therefore used the measured values of $\Delta\phi_-$ to determine Θ for $\Theta<0.4$ using the smooth curve as a reference. As a result the Ps fraction data display much less scatter in the region of low Li coverage.

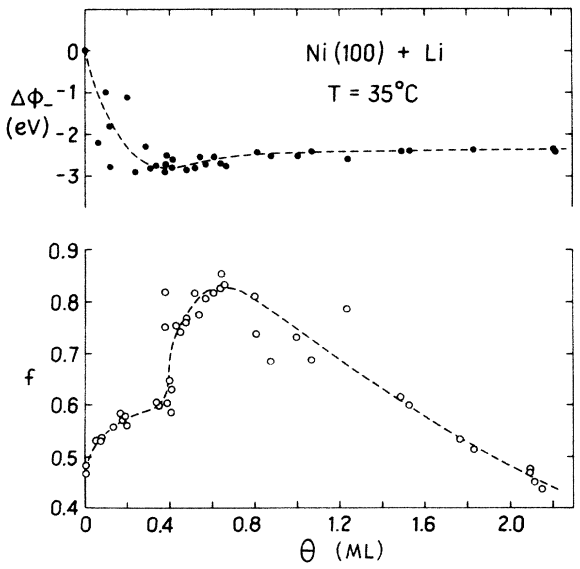

FIG. 10. Isothermal desorption of Ps and the change in electron work function, $\Delta\phi_-$, at $T=35$°C as the Li coverage is varied from 0 to 2.2 monolayers on Ni(100).

At low alkali coverage f increases initially for all surfaces. At submonolayer coverage where the alkali atom alters the surface dipole layer $\Delta\phi_-=-\Delta\phi_+$, and hence the Ps work function $\phi_{Ps}=\phi_-+\phi_+-6.8$ eV, should remain unchanged at about -3 eV. Thus the branching ratio of positrons into direct Ps formation should remain energetically favorable. The positron work function, which is -1.4 eV on Ni(100),[34] quickly becomes positive with alkali coverage. This turning off of bare positron emission, which competes with Ps formation, cannot however explain the initial rise in f since all emitted positrons are returned to the surface with a biased grid (see Fig. 1). As Θ increases fewer positrons must be captured by the surface state. Either the alkali atom reduces the capture rate into the surface state or emitted positrons returned to the surface preferentially fall into the surface state. This latter effect could only account for $df/d\Theta$ when $\Theta<0.1$, at which point positron emission is energetically no longer possible. However, all the Ni(100) data show a more complex behavior in f prior to the sharp rise near 0.5 monolayers. The Cs and clean K data go through a minimum whereas the Na and Li data appear to plateau before turning upward. Since this behavior may depend on such subtleties as impurities, trapping at surface defects in the alkali overlayer, or even detector systematics related to the velocity distribution of the emitted Ps, we will not consider it further.

At coverages above one monolayer one must consider the bulk properties of the alkali film. The bulk alkali metals, with ϕ_+ calculated[10] to be about 5 eV, are expected to have no bound positron surface state from which to desorb thermal Ps. In addition, the positronium work function, ϕ_{Ps}, for bulk Cs, Na, K, and Li are predicted[22] to be positive: 0.05 eV, 0.4 eV, 0.5 eV, and 1.3 eV, respectively. Thus all Ps emission, direct or thermal, should cease on bulklike alkali-metal samples in which the positrons are thermalized. However, in thin alkali-metal films the positrons that thermalized in the Ni substrate are propelled into (and presumably trapped) in the attractive overlayer. Unlike electronic states we must identify two positron "work functions" for this surface. The positron ground state in the Ni lies about 2 eV below the continuum (-1.4 eV $+3.5$ eV$=2.1$ eV), and 3 eV above the positron ground state for the bulk alkali metals ($\phi_+=5$ eV). Thus positrons crossing the Ni–alkali-metal interface may readily form Ps before inelastic processes can thermalize them in the film. As the film thickness is increased the fraction of Ps formed from nonthermal positrons should drop. Such a trend is

clearly evident in the Li data and this observation is consistent with the fact that Li is calculated to have the largest value of ϕ_{Ps} (1.3 eV) of all the alkali metals.[22] However, no reduction in f is observed near 3 monolayers coverage of Na and this may indicate that ϕ_{Ps} for bulk Na is actually negative. No clear trends can be discerned in the Cs and K data since only one monolayer is stable at 50 °C. Measurements with a cooled substrate would be required to further study ϕ_{Ps} and the rate of positron thermalization in these films.

VI. DISCUSSION

The data directly demonstrate that room-temperature thermal desorption of Ps from an alkali covered Ni surface occurs for $0.3 < \Theta < 0.5$. Assuming this trend continues at higher coverages, then we may conclude from Fig. 5 that E_a is a nearly linear function of Θ. From the viewpoint of the Born-Haber cycle [Eq. (1)] we might expect E_a to depend linearly on ϕ_- and hence only indirectly on the coverage Θ. To account for the universally measured slow variation of E_a on each surface when ϕ_- changes by 3 −3.5 eV, E_b has to rise by a comparable amount, as depicted in Fig. 11, to approximately 5 eV for each of the alkali-metal covered Ni surfaces investigated. If the surface state is viewed as originating from an image potential then this is indeed a surprising result. To date,[35] all positron surface binding energies have clustered around 2.5 ± 0.5 eV and, since the plasma frequency for the alkali metals is lower than for Ni, the expectation is that the binding energy should *decrease* with coverage. On the other hand, it might be possible to construct an *ad hoc* image-correlation potential in which the Ni substrate provides the repulsive barrier to entering the bulk and the alkali-metal film effectively broadens the correlation well—resulting in higher values of E_b. However, in such a model it is not clear how E_b could closely and universally mirror the behavior of ϕ_- as shown in Fig. 11.

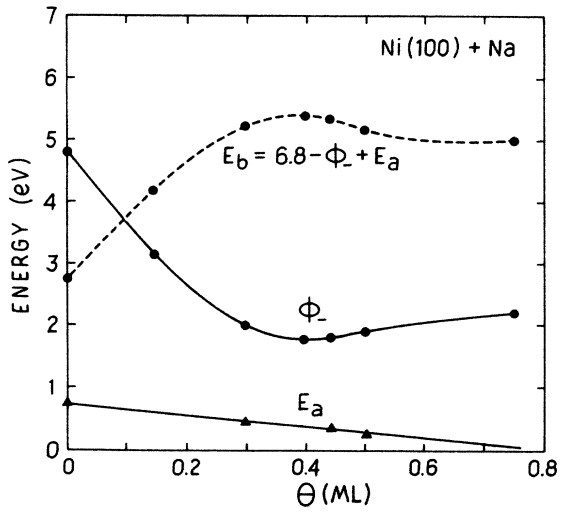

FIG. 11. The dashed curve is the required variation in the bare positron binding energy, E_b, determined from the values of E_a and ϕ_- as the Na coverage was varied on Ni(100).

Consequently the view of the positron surface state as originating from a bare positron and an image potential is qualitatively flawed. The fact that positrons in a relatively dilute electron gas have a much larger correlation energy than electrons suggests a strong difference in the character of the positron and electron surface states. Indeed, conceptually the physical desorption channel is via the desorption of Ps as a neutral, not positron, desorption. This is one of the attractions of the Ps physisorption model.[15] The desorbing particle is treated as a neutral particle and correlation is naturally incorporated by treating the surface bound particle as Ps. Qualitatively, the slow decrease in E_a with alkali-metal coverage is simply a manifestation of a weakening in the van der Waals potential as the surface plasma frequency decreases with coverage.

The detailed interaction between a positron and an inhomogeneous electron gas is a fundamentally difficult problem and we have considered a somewhat different approach to the problem. The questionable validity of the Born-Oppenheimer approximation for Ps prevents a rigorous decoupling of the Schrödinger equation into center-of-mass and relative coordinates. This complicates a chemical approach to the positron-surface interaction—where the center-of-mass coordinates are used as a parameter when solving for the electronic states. Still a tractable physical picture of the positron surface state is needed. Near the surface it involves a positron strongly correlated with the delocalized electrons of the metal. Far from the surface properly accounting for the interaction clearly requires a van der Waals potential. In between these regions we assume that the physical processes vary smoothly.

Platzman and Tzoar concentrate on the behavior of Ps far from the surface and extrapolate this van der Waals interaction to the repulsive surface barrier in their model of Ps physisorption to a metal surface.[15] They point out that, while physically appealing, this physisorption model represents an extreme opposite view to the image-bound positron. One problem with the model is that the van der Waals interaction for Ps depends critically on the $1s$-$2p$ promotion energy, which is assumed to be nearly constant over the region where a physisorption model is valid. Prior calculations of the $1s$ binding energy by Lowy and Jackson,[17] however, show the binding energy of this state to be decreased by several eV for an electron density as low as $r_s = 15$ and the $1s$ state to merge with the continuum at $r_s = 6.2$ (hence $E_{1s} - E_{2p} = 0$). The model also requires empirical parameters (i.e., a well depth cutoff and width) which depend on the short-range interaction of the Ps with the surface. A critical feature of the interaction between the positron and/or positronium and the metal surface is the qualitative change of the correlated electron from being bound in a Ps state to forming a screening cloud with the extended states of the metal. In the following development we concentrate on this latter aspect of the problem of the "near surface" interaction where Ps is energetically unfavorable. Conceptually we try to retain the

view of the positron plus the correlated electron as a neutral particle in a potential well.

The model used in discussing our results is based on the effective-medium theory[23] of Nørskov and Lang. In lowest order the effective-medium theory approximates the bonding of an atom to the inhomogeneous electron gas at the surface by embedding the atom in a homogeneous electron gas of density equal to that at the atoms core. The binding energy curve of the atom is then given by the variation of the electron density along the surface normal. The binding energy of the atom and the bond distance are identified with the minimum of the curve. The effective-medium theory has been found to accurately explain the weak dependence of hydrogen chemisorption on metals,[36] suggesting that a similar explanation may be found for our observed weak dependence of E_a on alkali-metal coverage.

We treat the bonding of Ps to the surface in a similar fashion, differing only where the low mass of Ps must be taken into account. First, the Ps $1s$ bound state merges into the continuum[17] for $r_s < 6.2$. Near the surface, where r_s is smaller than this critical value, we assume the electron correlation cloud crosses over from a localized Ps-like state to a screening cloud composed of extended states. Within a distance z of the surface the positron's correlation energy, E_c, with the inhomogeneous electron gas is approximated by that of a positron embedded in a homogeneous electron gas of density $\rho(z)$. The Thomas-Fermi screening length, l_F, is used to define the scaled variable $z^* = z/l_F$ (with $z^* = 0$ defined as the plane of the jellium edge). The variation of the electron density ρ with the distance is then determined using the "universal relation" of Rose, Smith, and Ferrante,[37]

$$\rho(z^*) = \begin{cases} \rho_0(1 - 0.54e^{1.04z^*}), & z^* < 0 \quad (5) \\ 0.46\rho_0 e^{-1.04z^*}, & z^* > 0. \quad (6) \end{cases}$$

With the above charge density and E_c from Ref. 24, the positron correlation potential can be constructed. Since the correlated particle is nearly neutral the surface dipole field does not enter in lowest order. Near the ion cores of the top layer a repulsive barrier is encountered where we turn on the full bulklike interaction of the positron-electron pair with the metal. The top of the barrier is taken to be $\phi_+ + \phi_-$ [$=3.4$ eV for Ni(100)] above the potential energy at large separation from the surface (similar to Ref. 15). Joining these potential energy curves yields not an effective-medium binding energy curve but a quantum well in which the composite particle is, presumably, trapped (as shown in the bottom curve of Fig. 12). The binding energy of this well for a particle of mass $2m_e$ then corresponds to the activation energy E_a for desorbing Ps. Solving the Schrödinger equation for such a potential indicates that the binding energy depends sensitively on the location of the repulsive inner potential step. For the clean Ni(100) surface we locate this step semi-empirically. We physically expect this inner potential step to occur somewhere between the plane containing the ion cores and the hollows

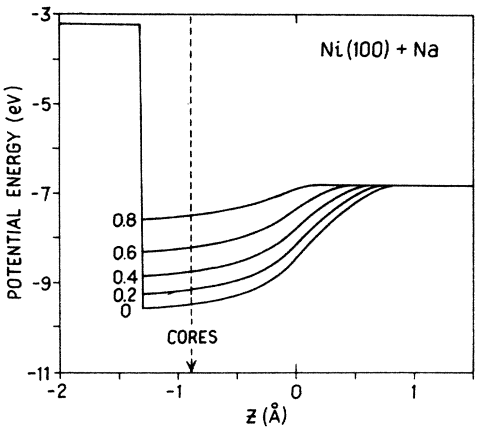

FIG. 12. Potential well calculated for various Na coverages, Θ, on Ni(100) formed by joining the correlation potential $E_c[\rho(z)]$ to the repulsive inner potential step at $z = -1.32$ Å. $z = 0$ is located at the jellium edge.

immediately below [$z = -0.88$ and -1.76 Å for Ni(100)]. The calculated binding energies are 0.10, 1.0, and 0.58 eV corresponding to locating the repulsive barrier at the two physical extremes and their midpoint (-1.32 Å). Given our experimental results (see Fig. 5) we select the intermediate value as the location of the potential step.

To calculate the effect of the alkali-metal overlayer on the binding energy we allow the bulk charge density and top layer core spacing, d, to linearly relax to the alkali values with Θ. Thus, for Na,

$$\rho(\Theta) = \rho_{\mathrm{Ni}} - (\rho_{\mathrm{Ni}} - \rho_{\mathrm{Na}})\Theta , \quad (7)$$

$$d(\Theta) = d_{\mathrm{Ni}} - (d_{\mathrm{Ni}} - d_{\mathrm{Na}})\Theta , \quad (8)$$

where we maintain the potential step at $0.75d$ ($= -1.32$ Å for $\Theta = 0$ and -1.58 Å for $\Theta = 1$). The resulting potential wells are shown in Fig. 12 for several coverages. The corresponding binding energies and the experimentally measured Ps activation energies are plotted in Fig. 13 versus Θ.

In this model the dominant effect of the alkali-metal overlayer is to weaken the correlation potential by reducing the charge density. Calculations performed without the d scaling relation [Eq. (8)] are similar (see Fig. 13). The calculated binding energies decrease in a linear fashion as do the measured activation energies. This trend is encouraging since linearly scaling ρ with Θ does not *a priori* imply a linear decrease in binding energy due to the dependence of the binding energy on the well shape and $E_c(\rho)$. In addition, the Na and Cs states are observed to be similar when plotted versus Θ and this is easily understood from Eq. (7). Since ρ_{Ni} is an order of magnitude larger than ρ_{Na} or ρ_{Cs}, the right-hand side of Eq. (7) is well approximated by $\rho_{\mathrm{Ni}}(1-\Theta)$ and hence only a weak dependence on the alkali-metal species is expected. This effect is also consistent with the observation that the steep increase in f in all the isothermal desorption curves (Figs. 6–10) occurs at the

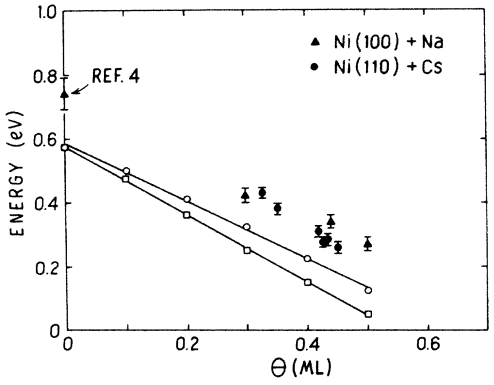

FIG. 13. The measured Ps activation energy, E_a, from Fig. 5 (solid symbols) replotted vs coverage, Θ (in monolayers). The open circles are the calculated binding energies of a composite particle of mass $2m_e$ in the model potential wells shown in Fig. 12 in which d was scaled with Θ using Eq. (8) (top curve) or held constant (lower curve). The calculated values are fitted to a straight line.

same coverage of approximately 0.5 monolayer.

Finally, we note that the agreement between theory and experiment in Fig. 13 is not perfect. While it was possible to tune the location of the step potential to fit the data more precisely, we felt this would be an overextension of such a simple lowest-order approximation. Clearly the presence of the strong dipole field at the surface will polarize the positron and its screening cloud, thus producing a greater attraction to the surface and a larger binding energy. Calculation of the first-order correction terms to account for the polarization are required. Furthermore, this lowest-order treatment will fail to account for the long surface state lifetime reported in Ref. 13. Higher-order polarization effects, which reduce the electron-positron overlap, may be able to account for this result.

VII. CONCLUSION

We conclude that the simplest interpretation of the alkali-metal results is that a strongly correlated positron is bound to the surface predominantly by a screening cloud composed of electrons from the extended states of the metal (primarily s and p states). The binding energy decreases with alkali-metal coverage as the correlation energy weakens due to the lower electron density outside the zero-pont barrier. A simple effective-medium treatment of these effects replicates the trends found in the data quite well. Such a treatment has several similarities with the approach employed by Cuthbert[20] using the hydrodynamic model and a single correlated electron. In both cases the center of mass of the composite polarized particle is much closer to the metal surface than would be the case for Ps physisorption. And, being close to the surface, the positron's screening cloud consists of delocalized metal states rather than a localized Ps bound state. It would be interesting to know if a hydrodynamic treatment could account for the effects of alkali-metal adsorption presented in this paper. Higher-order calculations in the effective-medium treatment are required to determine whether this model can quantitatively account for the observed long surface-state lifetime.

Further measurements should help clarify our understanding of positron surface states. Measurements on cooled surfaces would help substantiate the trend in E_a observed in Fig. 5. Angular correlation measurements on alkali-metal covered surfaces looking for the anticipated asymmetry[15] in the angular correlation of the annihilation γ rays should detect an increase in the Ps character of the surface state of these systems, if it exists. In addition, surface-state lifetime measurements on a variety of surfaces, including magnetized surfaces with spin polarized bound positrons (where spin averaging may not be applicable), should help resolve the question of the particular admixture of positron and positronium which is bound to a metal surface.

ACKNOWLEDGMENTS

We thank Kelvin Lynn, Allen Mills, Phil Platzman, and Arthur Rich for helpful discussions. This work has been supported by the National Science Foundation and the Office of the Vice President for Research of The University of Michigan. Two of us (D.W.G. and A.R.K.) gratefully recognize the hospitality and technical support of the General Motors Research Laboratories.

APPENDIX: SPIN POLARIZED MEASUREMENTS

In an earlier Letter[25] we showed that spin polarized positrons could probe the surface magnetic properties of Ni. We deduced the spin polarization of the electrons captured at the surface of Ni(110) to be $P_e = -2.5 \pm 0.3\%$, i.e., net majority spin. Since the Ni density of states is dominated by minority electrons near the Fermi energy, and since it is presumably these electrons that are principally captured in the Ps thermal desorption process, a large sign reversal in P_e would be expected when thermal desorption is occurring. However, on clean Ni the Ps desorption temperature (see Fig. 4) is 300–400 °C above the Curie temperature of 360 °C, and thus we have utilized Cs to reduce E_a and hence the desorption temperature. When the description temperature is reduced below the Ni Curie temperature, a definite strong preference for minority spins would be anticipated since the desorption process should strongly weight electrons within kT of the Fermi energy. As a result the thermally desorbed Ps may consist of almost 100% minority electrons. If true, such a surface would also be a highly efficient low-energy positron polarimeter.

Measurements of the triplet Ps formation asymmetry[26] on reversing either the positron spin polarization or the Ni magnetizing field were made at three coatings of Cs on Ni(110). The Cs-to-Ni Auger ratios of 0.03, 0.046, and 0.062 correspond to $\Theta = 0.2$, 0.3, and 0.4 monolayers, respectively. The corresponding values of f were 0.50, 0.58, and 0.79 indicating significant thermal desorption in the higher coverage run (see Fig. 6). However no significant asymmetry was measured for *any* of the three coverages. Either the Cs atoms modified the surface electronic structure to such an extent that the

surface magnetism was disrupted or the Ps formation process was altered so that a different distribution of electrons (perhaps a stronger weighting of *s* and *p*) participated in the screening and neutralization process. A similar quenching of the triplet Ps formation asymmetry had been previously observed[25] for a half monolayer of oxygen on Ni(110). Clearly, the electron capture process is highly surface sensitive, but a highly spin-selective process in Ps thermal desorption could not be observed in the present work.

*Present address: Department of Physics, Rice University, Houston, TX 77251

[1]K. G. Lynn, Phys. Rev. Lett. **43**, 391 (1979).
[2]A. P. Mills, Jr., Solid State Commun. **31**, 623 (1979).
[3]K. G. Lynn and D. O. Welch, Phys. Rev. B **22**, 99 (1980); K. G. Lynn and H. Lutz, *ibid.* **22**, 4143 (1980).
[4]I. J. Rosenberg, A. H. Weiss, and K. F. Canter, J. Vac. Sci. Technol. **17**, 253 (1980).
[5]S. Chu, A. P. Mills, Jr., and C. A. Murray, Phys. Rev. B **23**, 2060 (1981).
[6]P. M. Echenique and J. B. Pendry, J. Phys. C **11**, 2065 (1978).
[7]K. Giesen, F. Hage, F. J. Himpsel, H. J. Riess, and W. Steinmann, Phys. Rev. B **35**, 971 (1987) and references therein.
[8]C. H. Hodges and M. J. Stott, Solid State Commun. **12**, 1153 (1973).
[9]R. Nieminen and M. Manninen, Solid State Commun. **15**, 403 (1974).
[10]R. M. Nieminen and C. H. Hodges, Phys. Rev. B **18**, 2568 (1978).
[11]N. Barberan and P. M. Echenique, Phys. Rev. B **19**, 5431 (1979).
[12]R. M. Nieminen and M. J. Puska, Phys. Rev. Lett. **50**, 281 (1983); R. M. Niemimen, M. J. Puska, and M. Manninen, *ibid.* **53**, 1298 (1984).
[13]K. G. Lynn, W. E. Frieze, and P. J. Schultz, Phys. Rev. Lett. **52**, 1137 (1984).
[14]K. G. Lynn, A. P. Mills, R. N. West, S. Berko, K. F. Canter, and L. O. Roellig, Phys. Rev. Lett. **54**, 1702 (1985); R. H. Howell, P. Meyer, I. J. Rosenberg, and M. J. Fluss, *ibid.* **54**, 1698 (1985).
[15]P. M. Platzman and N. Tzoar, Phys. Rev. B **33**, 5900 (1986).
[16]A. R. Köymen, D. W. Gidley, and T. W. Capehart, Proceedings of the Workshop on Slow Positrons in Surface Science, Pajulahti, Finland, 1984 (unpublished).
[17]N. D. Lowy and A. D. Jackson, Phys. Rev. B **12**, 1689 (1975).
[18]J. R. Manson and R. H. Ritchie, Phys. Rev. B **29**, 1084 (1984).
[19]G. Barton, J. Phys. C **15**, 4727 (1982) and earlier work referenced therein.
[20]A. Cuthbert, J. Phys. C **18**, 4561 (1985).
[21]A. P. Mills, Jr., and Loren Pfeiffer, Phys. Rev. Lett. **43**, 1961 (1979).
[22]R. M. Nieminen and J. Oliva, Phys. Rev. B **22**, 2226 (1980).
[23]J. K. Nørskov and N. D. Lang, Phys. Rev. B **21**, 2131 (1980).
[24]P. Bhattacharyya and K. S. Singwi, Phys. Lett. **41A**, 457 (1972); see also Ref. 17, J. Arponen and E. Pajanne, Ann. Phys. **121**, 343 (1979), and P. Pietiläinen and A. Kallie, Phys. Rev. B **27**, 224 (1983).
[25]D. W. Gidley, A. R. Köymen, and T. W. Capehart, Phys. Rev. Lett. **49**, 1779 (1982).
[26]A. R. Köymen, Ph. D. thesis, The University of Michigan, 1984.
[27]D. R. Penn, J. Electron Spectrosc. Relat. Phenom. **9**, 29 (1976).
[28]R. L. Gerlach and T. N. Rhodin, Surf. Sci. **17**, 32 (1969).
[29]S Andersson and V. Jostell, Surf. Sci. **46**, 625 (1974).
[30]R. L. Gerlach and T. N. Rhodin, Surf. Sci. **19**, 403 (1970).
[31]C. A. Papageorgopoules and J. M. Chen, Surf. Sci. **52**, 40 (1974).
[32]D. W. Gidley and P. W. Zitzewitz, Phys. Lett. **69A**, 97 (1978).
[33]A. P. Mills, Jr., Loren Pfeiffer, and P. M. Platzman, Phys. Rev. Lett. **51**, 1085 (1983).
[34]D. M. Fischer, K. G. Lynn, and D. W. Gidley, Phys. Rev. B **33**, 4479 (1986).
[35]For a compilation of results, see A. P. Mills, Jr. in *Proceedings of Interational School of Physics, "Enrico Fermi," Course* LXXIII, *Varenna, 1981,* edited by W. Brandt and A. Dupasquier (Academic, New York, 1982).
[36]P. Nordlander, S. Holloway, and J. K. Nørskov, Surf. Sci. **136**, 59 (1984).
[37]James H. Rose, John R. Smith, and John Ferrante, Phys. Rev. B **28**, 1835 (1983).

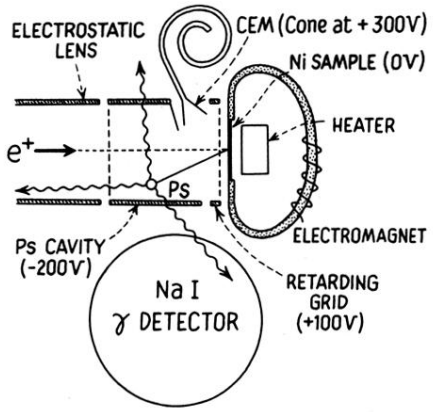

FIG. 1. Schematic diagram of the experimental arrangement showing the electrostatic lenses, Ps cavity, sample holder, γ detector, and channel electron multiplier (CEM).